# On Mathematical Modelling of Flow Induced Vocal Folds Vibrations During Phonation

**Petr Sváček**

**Abstract** In this paper the problem of mathematical modelling of phonation is discussed. The main attention is paid to the treatment of vocal fold vibrations including the periodical appearance of their contacts. A simplified mathematical model is presented, numerically analyzed and discussed. The Hertz impact forces are used in the structural part. In order to treat the contact phenomena in the fluid model a strategy based on fictitious porous media is introduced. The numerical discretization is described and numerical results are presented.

**Keywords** Aeroelasticity · Navier-Stokes equations · Finite element method

## 1 Introduction

The fluid-structure-acoustic interaction problems are usually associated with technical applications as aeroelasticity, see [1]. However, couplings between fluid flow, elastic structure deformation and acoustics are involved also in biomechanics of voice, see [2]. Voice production is a complex process, which involves airflow induced vibrations of vocal folds generating a sound source. The fundamental sound is further modified by the acoustic resonances in the vocal tract cavities. The vocal folds start to oscillate at the so-called phonation onset (flutter instability) given by certain airflow rate and a certain prephonatory vocal folds position, see [3]. For higher flow rates, the glottis is closing during VFs vibration and the VFs collide loading the tissue periodically by the contact stress. Consequently, the mathematical modelling of phonation process is challenging task, it addresses flow field, structure deformation as well as acoustics, see e.g. [4].

The financial support was provided by the *Czech Science Foundation* under the *Grant No. 19-04477S*.

P. Sváček (✉)
Faculty of Mechanical Engineering, Department of Technical Mathematics, Czech Technical University in Prague, Karlovo nám. 13, 121 35 Praha 2, Czech Republic
e-mail: Petr.Svacek@fs.cvut.cz



F. Yilmaz et al. (eds.), *Mathematical Methods for Engineering Applications*,
Springer Proceedings in Mathematics & Statistics 384,
https://doi.org/10.1007/978-3-030-96401-6_20

In this paper an attention is paid the mathematical modelling of the voice production. As during voice creation the airflow velocity in the human glottal region is lower than 100 m/s, one can use separately the incompressible Navier-Stokes model for the fluid flow and the Lighthill's acoustic analogy for the acoustic wave propagation, see [5]. The considered problem is characterized as a problem of fluid-structure interaction and an attention is paid to the problem of glottis closure (glottis is the narrowest part between the vibrating vocal folds).

Computational modelling can help with analysis of the physical background of the phonation processes. These involve the interactions of the fluid flow with solid body deformation, the contact problem and acoustics. One of the possible approaches is using of a simplified model as the 2-mass model of the vocal folds of [6], where a simplified air flow model is used. Such aeroelastic models [3] has applications in simulation of vowels and in estimation of the vocal fold loading by impact stress and inertial forces.

Here, a simplified lumped VF model with the Hertz contact model is considered in order to more easily address the phenomena of fluid-structure interactions with the contact of the vibrating structure similarly as in [7] and [8]. Due to the same reason a suitable modification of the inlet boundary condition is used. The novelty of this paper lies in verification of the problem formulation with modified boundary conditions, where a simplified stationary model problem is analyzed. Further, more consistent formulation of the porous media term is used in the present paper compared to the approach proposed in [7]. The applied numerical method is described and numerical results are shown.

## 2 Mathematical Model

We consider two-dimensional model of incompressible fluid flow in an interaction with a simplified model of vocal fold, whose deformation is described as motion of an equivalent mechanical systems with two-degrees of freedom, see [3].

### *2.1 Flow Model*

First, the flow model through the two dimensional model of the computational domain $\Omega_t$ during the phonation onset phase is introduced. In this case only small amplitudes of the vibrations of vocal folds appear and thus the flow in the domain $\Omega_t$ can be treated with the aid of Arbitrary Lagrangian Eulerian (ALE) method, see [9]. The computational domain $\Omega_t$ is shown at Fig. 1, where the additional assumption of a symmetric flow and symmetric vibrations of vocal folds are made. The boundary $\partial\Omega_t$ is assumed to consist of the inlet $\Gamma_I$, the outlet $\Gamma_O$, the axis of symmetry $\Gamma_S$ and the time dependent part of boundary $\Gamma_t$ consisting of its fixed $\Gamma_F$ and deformable part $\Gamma_{Wt}$, which corresponds to the surface of the vibrating vocal fold.

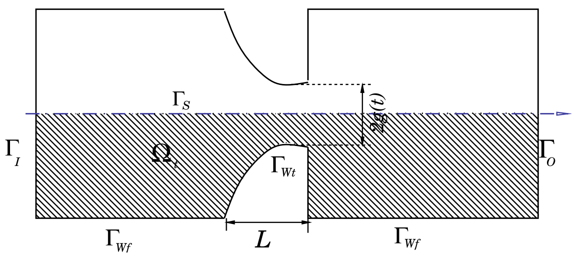


**Fig. 1** The computational domain $\Omega_t$ with specification of the boundary parts

The flow in the computational domain $\Omega_t$ is modelled as incompressible fluid flow described by the system of the incompressible Navier-Stokes equations (cf. [10]) written in the ALE form.

$$\frac{D^{\mathcal{A}}\boldsymbol{u}}{Dt} + ((\boldsymbol{u} - \boldsymbol{w}_D) \cdot \nabla)\boldsymbol{u} = \text{div}\boldsymbol{\tau}^f, \\ \nabla \cdot \boldsymbol{u} = 0, \tag{1}$$

where $\boldsymbol{u}$ denotes the fluid velocity vector $\boldsymbol{u} = (u_1, u_2)$, $\boldsymbol{\tau}^f = (\tau_{ij}^f)$ is the fluid stress tensor given as $\boldsymbol{\tau}^f = -p\mathbb{I} + \nu\left(\nabla\boldsymbol{u} + \nabla^T\boldsymbol{u}\right)$, $p$ is the kinematic pressure (means pressure divided by the constant fluid density $\rho$) and $\nu > 0$ denotes the constant kinematic fluid viscosity (the viscosity divided by the density). Further, $\boldsymbol{w}_D$ denotes the domain velocity (i.e. the velocity of the point with a fixed reference), and $\frac{D^{\mathcal{A}}\boldsymbol{u}}{Dt}$ is the ALE derivative, i.e. the derivative with respect to the reference configuration $\Omega_{ref}$. Both the domain velocity $\boldsymbol{w}_D$ as well as the ALE derivative depends on the ALE mapping $\mathcal{A}_t$ describing the deformation of a reference domain $\Omega_{ref}$ onto the computational domain $\Omega_t$.

The system (1) is then equipped with an initial condition and with the following boundary conditions are prescribed

$$\begin{aligned}
&\text{(a) } \boldsymbol{u} = \boldsymbol{w}_D \text{ on } \Gamma_{Wt}, \\
&\text{(b) } u_2 = 0, -\tau_{12}^f = 0 \text{ on } \Gamma_S, \\
&\text{(c) } \frac{1}{2}(\boldsymbol{u}\cdot\boldsymbol{n})^-\boldsymbol{u} - \boldsymbol{n}\cdot\boldsymbol{\tau}^f = \frac{1}{\varepsilon}(\boldsymbol{u} - \boldsymbol{u}_I) \text{ on } \Gamma_I, \\
&\text{(d) } \frac{1}{2}(\boldsymbol{u}\cdot\boldsymbol{n})^-\boldsymbol{u} - \boldsymbol{n}\cdot\boldsymbol{\tau}^f = p_{ref}\boldsymbol{n} \text{ on } \Gamma_O,
\end{aligned} \tag{2}$$

where $\boldsymbol{u}_I$ is a given reference inlet velocity, $p_{ref}$ is a reference outlet pressure, $\boldsymbol{n}$ denotes the unit outward normal vector to $\partial\Omega_t^f$, $\alpha^-$ denotes the negative part of a real number $\alpha$. Here, the boundary condition (2c) weakly imposes the inlet velocity $\boldsymbol{u}_I$ using the penalization parameter $\varepsilon > 0$.

## 2.2 Vocal Fold Vibrations

The vocal fold vibrations is modelled using the mechanically equivalent two degrees of freedom model characterized by three masses $m_1$, $m_2$ and $m_3$. The two masses $m_1$ and $m_2$ are displaced by the length $l = L/2$ from the center of the vocal fold, where the mass $m_3$ is located. The three masses $m_1, m_2, m_3$ were determined by

$$m_{1,2} = \frac{1}{2l^2}(I + m\,e^2 \pm m\,e\,l), \qquad m = m_1 + m_2 + m_3, \tag{3}$$

with $l = L/2$ being the distance of the masses $m_1$ and $m_2$ from the center, $m$ denotes the total mass $m = m_1 + m_2 + m_3$, $e$ is the eccentricity and $I$ is the inertia moment, see Fig. 2. The parameters $e$, $m$ and $I$ are determined using the density $\rho_{VF} = 1020$ kg/m$^3$, the length (depth of the channel in the third dimension) $h = 18$mm and the (parabolic) shape of the surface of the vocal fold

$$a_m(x) = 1.858\,x - 159.861\,x^2 \text{ [m]} \tag{4}$$

for $x \in \langle 0, L\rangle$ [m] with $L$ being the thickness of the vocal fold $L = 6.8$ mm.

The vibration of the vocal fold is modelled by two degrees of freedom, see Fig. 2, which are the displacements $w_1(t)$ and $w_2(t)$ of the masses $m_1$ and $m_2$, respectively. The governing equation of motion reads

$$\mathbb{M}\ddot{\boldsymbol{w}} + \mathbb{B}\dot{\boldsymbol{w}} + \mathbb{K}\boldsymbol{w} = -\boldsymbol{F}, \tag{5}$$

where $\mathbb{M}$ is the mass matrix of the system, $\mathbb{K}$ is the stiffness matrix of the system characterized by the spring constants $k_1, k_2$, see [3] for details. The matrices are given by

$$\mathbb{M} = \begin{pmatrix} m_1 + \frac{m_3}{4} & \frac{m_3}{4} \\ \frac{m_3}{4} & m_2 + \frac{m_3}{4} \end{pmatrix}. \quad \mathbb{K} = \begin{pmatrix} k_1 & 0 \\ 0 & k_2 \end{pmatrix}, \quad \mathbb{B} = \varepsilon_1\mathbb{M} + \varepsilon_2\mathbb{K} \tag{6}$$

The vector $\boldsymbol{F} = \boldsymbol{F}_{imp} + \boldsymbol{F}_{aero}$ consists of the impact forces $\boldsymbol{F}_{imp}$ and the aerodynamical forces $\boldsymbol{F}_{aero} = (F_1, F_2)^T$ (downward positive) acting at the masses $m_1$ and $m_2$

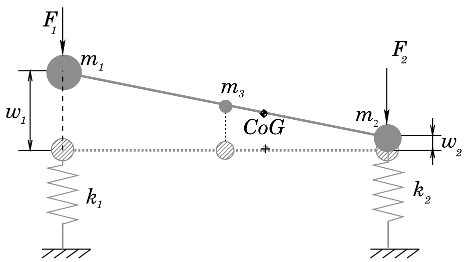


**Fig. 2** Two degrees of freedom model (with masses $m_1, m_2, m_3$) in displaced position (displacements $w_1$ and $w_2$). The acting aerodynamic forces $F_1$ and $F_2$ are shown

evaluated from the aerodynamical forces as surface integrals using the (kinematic) pressure $p$ and derivatives flow velocity $\boldsymbol{u} = (u_1, u_2)$, see [7].

Moreover, the displacement of the structure surface $\Gamma_{Wt}$ determines the boundary condition for the construction of the ALE mapping and the domain velocity $\boldsymbol{w}_D$ at $\Gamma_{Wt}$ is determined using by time derivatives of $w_1, w_2$.

## 2.3 Contact Problem

The treatment of the contact the vocal folds in the flow model requires to address not only the inlet boundary condition, but also the periodical topological changes of the flow domain. It can be realized more easily for the simplified situation of the symmetric domain, but this concept can be extended to a more complicated case. First, in this section the computational domain $\Omega_t$ is assumed to be formed of the subdomain $\Omega_t^f$, which is really occupied by the fluid(air), and the subdomain $\Omega_t^p$, which is still part of the computational flow domain but it should be occupied the elastic vocal fold $\Omega_t^{VF}$. In practical implementation, the domain $\Omega_t^p$ is determined as the intersection of the domain $\Omega_t$ with the deformed vocal fold domain $\Omega_t^{VF}$. The geometrical modification of the motion of the surface $\Gamma_{Wt}$ is based on the deformation of the surface at the contact region, see Fig. 3, where the deformation is locally modified not to violate the minimal gap condition. At these points the surface of the vocal fold is shifted in order to guarantee the minimal gap ($g_{min}$) condition, see Fig. 3.

The part of the fluid domain $\Omega_t^p$ is assumed to be domain of porous media, and the flow is then assumed to be governed by the modified equations

$$\frac{D^{\mathcal{A}}\boldsymbol{u}}{Dt} + ((\boldsymbol{u} - \boldsymbol{w}_D) \cdot \nabla)\boldsymbol{u} + \boldsymbol{\sigma}_P \boldsymbol{u} = \text{div}\boldsymbol{\tau}^f, \tag{7}$$

where the tensor coefficient $\boldsymbol{\sigma}_P$ corresponds to the artificial porosity of the fictitious porous media, see [11], or it can be understand as penalization, see [12]. Here the tensor is chosen to act only the x-direction, i.e. the choice $\boldsymbol{\sigma}_P = \frac{P}{\nu}\boldsymbol{e}_1 \otimes \boldsymbol{e}_1 \chi_{\Omega_t^p}$ was used,

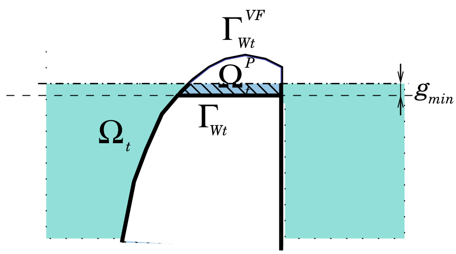


**Fig. 3** The detail of the porous media flow domain $\Omega_t^p$

where $P$ denotes the artificial porosity coefficient and $\chi_{\Omega_t^p}$ denotes the characteristic function of the set $\Omega_t^p$ which is equal to one on $\Omega_t^p$ and zero otherwise.

Although this approach can be written generally, for the presented model problem it can be described more specifically: The reference (undeformed) shape of the vocal fold $\Omega_{ref}^{VF}$ is given by

$$\Omega_{ref}^{VF} = \{[x, y] \in \mathbb{R}^2 : x \in (0, L), -H < y < a_m(x) - H\}, \tag{8}$$

where $H = g_0 + H_{VF}$ denotes the half-height of the inlet channel given as sum of the initial halfgap $g_0$ and the height of the vocal fold $H_{VF} = \max_{x \in [0,L]} a_m(x)$. The deformation of the vocal fold $\Omega_t^{VF}$ is described using $w_1, w_2$ by the Lagrangian mapping $\mathcal{L}_t(x, y) = (x, y_{new})$ with

$$y_{new} = y + \frac{w_1 + w_2}{2} + \frac{w_2 - w_1}{L} x \tag{9}$$

for $[x, y] \in \Omega_{ref}^{VF}$. In particularly, the position of the vocal fold surface $\Gamma_t^{VF}$ (interface between the fluid and structure domain) is given as

$$\Gamma_t^{VF} = \{[x, y] \in \mathbb{R}^2 : x \in [0, L], y = a_m(x) - H + \frac{w_1 + w_2}{2} + \frac{w_2 - w_1}{L} x\}. \tag{10}$$

The domain $\Omega_t^P$ can be characterized as all points $[x, y] \in \Omega_t^{VF}$ which would violate the condition $g(t) \geq g_{min}$ or $y > -g_{min}$. Consequently, the porous media domain can be specified as

$$\Omega_t^p = \{[x, y] \in \mathbb{R}^2 : x \in (0, L), -g_{min} < y < a_m(x) - H + \frac{w_1 + w_2}{2} + \frac{w_2 - w_1}{L} x\}, \tag{11}$$

see Fig. 3.

Let us mention, that for the half-gap $g(t)$ (i.e. the oriented distance of the vocal fold and the symmetry axis) satisfying $g(t) \geq g_{min} > 0$ (phonation onset) such an intersection is naturally empty and in this case the mathematical model is equivalent to the mathematical model presented in [15] and the presented numerical method then leads to the same results, which well determines the flutter velocity.

## 3 Existence and Uniqueness of a Stationary Solution

In order to discuss the penalization boundary condition we shall start with a simplified stationary problem on two-dimensional domain $\Omega \subset \mathbb{R}^2$ with the Lipschitz-continuous boundary $\partial\Omega$. The system of Navier-Stokes equations is written in the form

$$
\begin{aligned}
-\nu\triangle u_i + \boldsymbol{u}\cdot\nabla u_i + \frac{\partial p}{\partial x_i} = f_i, \qquad i = 1,2, \quad \text{in } \Omega \\
\nabla\cdot\boldsymbol{u} = 0, \quad \text{in } \Omega
\end{aligned} \tag{12}
$$

with the boundary conditions prescribed on the mutually disjoint parts $\partial\Omega = \Gamma_0 \cup \Gamma_1 \cup \Gamma_2 \cup \Gamma_S$, as

$$
\begin{aligned}
\boldsymbol{u} = 0, \qquad & \text{on } \Gamma_0, \\
-\nu\frac{\partial \boldsymbol{u}}{\partial \boldsymbol{n}} + (p - p_{ref})\boldsymbol{n} - \frac{1}{2}(\boldsymbol{u}\cdot\boldsymbol{n})^-\,\boldsymbol{u} = 0, \qquad & \text{on } \Gamma_1 \cup \Gamma_2,
\end{aligned} \tag{13}
$$

with $p_{ref} = p_i$ on $\Gamma_i$, $i = 1, 2$.

The stationary problem of Navier-Stokes system of equations reads: Find $\boldsymbol{u} \in \mathcal{X}$ such that for all $\boldsymbol{z} \in \mathcal{X}$ and $q \in \mathcal{Q}$

$$
\begin{aligned}
\nu\Big(\nabla\boldsymbol{u}, \nabla\boldsymbol{z}\Big)_\Omega + c(\boldsymbol{u};\boldsymbol{u},\boldsymbol{z}) - \Big(p, \nabla\cdot\boldsymbol{z}\Big)_\Omega + \Big(q, \nabla\cdot\boldsymbol{u}\Big)_\Omega + \\
+ \int\limits_{\Gamma_1\cup\Gamma_2} \frac{1}{2}(\boldsymbol{u}\cdot\boldsymbol{n})^+\boldsymbol{u}\cdot\boldsymbol{z}\,dS = \Big(\boldsymbol{f}, \boldsymbol{z}\Big)_\Omega - \sum_{k=1}^{2}\int_{\Gamma_k} p_k(\boldsymbol{z}\cdot\boldsymbol{n})\,dS.
\end{aligned} \tag{14}
$$

In order to prove the existence and uniqueness of the solution let us consider the subspace $\mathcal{X}_{div} \subset \mathcal{X}$ defined as

$$
\mathcal{X}_{div} = \{\boldsymbol{\varphi} \in \mathcal{X}, \nabla\cdot\boldsymbol{\varphi} = 0\}.
$$

Any solution $\boldsymbol{u} \in \mathcal{X}$ of Equation (14) satisfies $\boldsymbol{u} \in \mathcal{X}_{div}$ and moreover the equation

$$
\nu\Big(\nabla\boldsymbol{u}, \nabla\boldsymbol{z}\Big)_\Omega + c(\boldsymbol{u};\boldsymbol{u},\boldsymbol{z}) + \int\limits_{\Gamma_1\cup\Gamma_2} \frac{1}{2}(\boldsymbol{u}\cdot\boldsymbol{n})^+\boldsymbol{u}\cdot\boldsymbol{z}\,dS = \Big(\boldsymbol{f}, \boldsymbol{z}\Big)_\Omega - (p_1 - p_2)\int_{\Gamma_1}(\boldsymbol{z}\cdot\boldsymbol{n})\,dS. \tag{15}
$$

holds for all $\boldsymbol{z} \in \mathcal{X}_{div}$.

**Theorem 1** (Existence and uniqueness of the solution) *Let $C_F\|\boldsymbol{f}\|_{0,2,\Omega} + C_1|p_2 - p_1| < \frac{\nu^2}{\widetilde{C}}$, where $C_F$ is the constant from Friedrichs inequality, $C_1$ is the constant from the trace theorem and $\widetilde{C}$ is the constant from the continuity of the trilinear form c. Then there exists an unique solution $\boldsymbol{u} \in \mathcal{X}_{div}$, which satisfies Equation (15) for all $\boldsymbol{z} \in \mathcal{X}_{div}$.*

***Proof*** 1. First, we consider for any $\boldsymbol{w} \in \mathcal{X}_{div}$ the problem: find $\boldsymbol{u} \in \mathcal{X}_{div}$

$$
\mathcal{A}_{\boldsymbol{w}}(\boldsymbol{u}, \boldsymbol{z}) = \mathcal{L}(\boldsymbol{z}) \qquad \text{for all } \boldsymbol{z} \in \mathcal{X}_{div}.
$$

The bilinear form $\mathcal{A}_{\boldsymbol{w}}(\cdot,\cdot)$ is defined by

$$\mathcal{A}_{\boldsymbol{w}}(\boldsymbol{u}, z) = \nu\Big(\nabla \boldsymbol{u}, \nabla z\Big)_{\Omega} + c(\boldsymbol{u}; \boldsymbol{u}, z) + \int_{\Gamma_1 \cup \Gamma_2} \frac{1}{2}(\boldsymbol{u} \cdot \boldsymbol{n})^{+} |\boldsymbol{u}|^2 dS,$$

and the form $\mathcal{L}(\cdot)$ is defined by

$$\mathcal{L}(z) = \Big(\boldsymbol{f}, z\Big)_{\Omega} - (p_1 - p_2) \int_{\Gamma_1} (z \cdot \boldsymbol{n}) dS,$$

because for any $z \in \mathcal{X}_{div}$ holds

$$\sum_{k=1}^{2} \int_{\Gamma_k} p_k (z \cdot \boldsymbol{n}) dS = (p_1 - p_2) \int_{\Gamma_1} (z \cdot \boldsymbol{n}) dS.$$

The bilinear form $\mathcal{A}_{\boldsymbol{w}}(\cdot, \cdot)$ is continuous and coercive on $\mathcal{X}_{div}$, the linear form $\mathcal{L}(\cdot)$ is continuous on $\mathcal{X}_{div}$. Thus for any $\boldsymbol{w}^* \in \mathcal{X}_{div}$ there exists solution $z^* \in \mathcal{X}_{div}$ such that

$$\mathcal{A}_{\boldsymbol{w}^*}(z^*, z) = \mathcal{L}(z) \qquad \text{for all } z \in \mathcal{X}_{div}.$$

With the choice of $z = z^*$ we get the following apriori bound

$$\nu |z^*|_{1,\Omega}^2 \leq \mathcal{A}_{\boldsymbol{w}}(z^*, z^*) = \mathcal{L}(z^*) \leq \Big(C_F \|\boldsymbol{f}\|_{0,2,\Omega} + C_1 |p_2 - p_1|\Big) |z^*|_{1,\Omega}$$

thus

$$|z^*|_{1,\Omega} \leq \frac{1}{\nu}\Big(C_F \|\boldsymbol{f}\|_{0,2,\Omega} + C_1 |p_2 - p_1|\Big).$$

2. We define the mapping $\Psi : \boldsymbol{w} \to z$ from $\mathcal{K}$ onto $\mathcal{K}$, where

$$\mathcal{K} = \left\{ z \in \mathcal{X}_{div}, |z|_{1,\Omega} \leq \frac{1}{\nu}\Big(C_F \|\boldsymbol{f}\|_{0,2,\Omega} + |p_2 - p_1| C_1\Big) \right\},$$

where $C_1$ is the constant from the trace theorem. Further, we will show that the mapping $\Psi$ is the contractive mapping on $\mathcal{K}$. Let us take $\boldsymbol{w}_1, \boldsymbol{w}_2 \in \mathcal{K}$ and denote $z_1 = \Psi(\boldsymbol{w}_1)$ and $z_2 = \Psi(\boldsymbol{w}_2)$. Thus the following equations are satisfied

$$\begin{aligned} \mathcal{A}_{\boldsymbol{w}_1}(z_1, z_2 - z_1) &= \mathcal{L}(z_2 - z_1), \\ \mathcal{A}_{\boldsymbol{w}_2}(z_2, z_2 - z_1) &= \mathcal{L}(z_2 - z_1). \end{aligned}$$

Now by subtracting both equations we get from the continuity of the trilinear form $c$

$$\begin{aligned} \nu |z_2 - z_1|_{1,\Omega}^2 &= c(\boldsymbol{w}_2 - \boldsymbol{w}_1; z_2, z_2 - z_1) \\ &\leq \tilde{C} |\boldsymbol{w}_2 - \boldsymbol{w}_1|_{1,\Omega} |z_2|_{1,\Omega} |z_2 - z_1|_{1,\Omega} \end{aligned}$$

and with $z_2 \in \mathcal{K}$ we have

$$|z_2 - z_1|^2_{1,\Omega} \leq \frac{\tilde{C}}{\nu^2}\Big(C_F \|\boldsymbol{f}\|_{0,2,\Omega} + |p_2 - p_1|C_1\Big)|\boldsymbol{w}_2 - \boldsymbol{w}_1|_{1,\Omega}.$$

Thus the mapping $\Psi$ is a contractive mapping from $\mathcal{K}$ in $\mathcal{K}$, and there exists a fixed point of the mapping $\Psi$, which is the unique solution of the problem (15).

## 4 Numerical Approximation

In this section the numerical approximation of the flow model is introduced: an equidistant partition $t_j = j\Delta t$ of the time interval $I$ with a constant time step $\Delta t > 0$ is considered. At time instants $t_j$, $j = 0, 1, \ldots$ the approximations of velocity and pressure are sought $\boldsymbol{u}^j \approx \boldsymbol{u}(\cdot, t_j)$ and $p^j \approx p(\cdot, t_j)$, respectively. The domain velocity at time instant $t_j$ is denoted by $\boldsymbol{w}_D^j$. For the time discretization the formally second order backward difference formula is used, i.e. the ALE derivative is approximated at $t = t_{n+1}$ as

$$\frac{D^{\mathcal{A}}\boldsymbol{u}}{Dt}\Big|_{t_{n+1}} \approx \frac{3\boldsymbol{u}^{n+1} - 4\tilde{\boldsymbol{u}}^n + \tilde{\boldsymbol{u}}^{n-1}}{2\Delta t} \tag{16}$$

where at a given time instant $t = t_{n+1}$ by $\tilde{\boldsymbol{u}}^k$ the transformation of the velocity $\boldsymbol{u}^k$ defined on $\Omega_{t_k}$ onto $\Omega_{t_{n+1}}$ is denoted.

In order to apply finite element method the weak form of Eqs. (1) is derived in a standard form, where the ALE derivative is approximated using Eq. (16). The stabilized weak at time instant $t_{n+1}$ form then reads: find finite element approximations $U = (\boldsymbol{u}, p) := (\boldsymbol{u}^{n+1}, p^{n+1})$ such that $\boldsymbol{u}$ satisfy the boundary condition (2a) and

$$a(U; U, V) + a_S(U; U, V) + \mathcal{P}_S(U, V) = L(V) + L_S(V) \tag{17}$$

holds for any test functions $V = (z, q)$ from the finite element spaces, [7] for details. The Galerkin forms $a$ and $L$ are defined for any $U = (\boldsymbol{u}, p)$, $\overline{U} = (\overline{\boldsymbol{u}}, \overline{p})$ and $V = (z, q)$ by

$$\begin{aligned} a(\overline{U}; U, V) = &\int_\Omega \left( (\frac{3}{2\Delta t} + \boldsymbol{\sigma}_P)\boldsymbol{u} + ((\overline{\boldsymbol{w}} \cdot \nabla)\boldsymbol{u} \right) \cdot z dx - \int_{\Gamma_{I,O}} \frac{1}{2}(\overline{\boldsymbol{u}} \cdot \boldsymbol{n})^- \boldsymbol{u} \cdot z dS \\ &+ \int_{\Gamma_I} \frac{1}{\varepsilon}\boldsymbol{u} \cdot z dS + \int_\Omega (2\nu(\nabla\boldsymbol{u} : \nabla z) - (\nabla \cdot z)p)\, dx \end{aligned} \tag{18}$$

and

$$L(V) = \int_\Omega \frac{4\tilde{\boldsymbol{u}}^n - \tilde{\boldsymbol{u}}^{n-1}}{2\Delta t} \cdot z dx + \int_{\Gamma_I} \frac{1}{\varepsilon}\boldsymbol{u}_I \cdot z dS - \int_{\Gamma_O} p_{ref}(\boldsymbol{n} \cdot z) dS, \tag{19}$$

where $\overline{\boldsymbol{w}} = \overline{\boldsymbol{u}} - \boldsymbol{w}_D^{n+1}$, $\Omega := \Omega_{t_{n+1}}$.

The terms $a_S(U; U, V)$ and $L_S(U; V)$ are the SUPG/PSPG stabilization terms and the term $\mathcal{P}_S$ denotes the div-div stabilization term. The stabilization terms are defined locally on each element $K$ of the employed triangulation $\mathcal{T}_\Delta$ and summed together, i.e.

$$
\begin{aligned}
a_S(\overline{U}; U, V) &= \sum_{K\in\mathcal{T}_\Delta} \delta_K \left( (\frac{3}{2\Delta t} + \boldsymbol{\sigma}_P)\boldsymbol{u} - \mu\Delta\boldsymbol{u} + (\overline{\boldsymbol{w}}\cdot\nabla)\,\boldsymbol{u} + \nabla p, (\overline{\boldsymbol{w}}\cdot\nabla)z + \nabla q \right)_K \\
L_S(\overline{U}; V) &= \sum_{K\in\mathcal{T}_\Delta} \delta_K \left( \frac{4\tilde{\boldsymbol{u}}^n - \tilde{\boldsymbol{u}}^{n-1}}{2\Delta t}, (\overline{\boldsymbol{w}}\cdot\nabla)z + \nabla q \right)_K \\
\mathcal{P}_S(U, V) &= \sum_{K\in\mathcal{T}_\Delta} \tau_K \Big( \nabla\cdot\boldsymbol{u}, \nabla\cdot z \Big)_K,
\end{aligned}
$$

where $\delta_K$, $\tau_K$ are stabilization parameters chosen similarly as in [15].

The problem (17) is linearized, strongly coupled with the structural solver and the described treatment of the contact problem is used.

## 5 Numerical Results

This section presents the numerical results for the described aeroelastic model. The parabolic vocal fold shape $a_m(x)$ given by Eq. (4) was used and the computations with the initial half-gap chosen as $g_0 = 0.2$mm and the inflow velocity $U_\infty = 0.65 m/s$ were performed. These conditions the phonation onset occurs, see [15]. The following parameters were used: the mass $m = 4.812 \times 10^{-4}$ kg, the inertia moment $I = 2.351 \times 10^{-9}$ kg / m$^2$ and the eccentricity $e = 0.771 \times 10^{-3}$ m. The stiffness constants were chosen as $k_1 = 56$N/m and $k_2 = 174.3$ N/m. The proportional damping constants were set to $\varepsilon_1 = 120.35\,\text{s}^{-1}$ and $\varepsilon_2 = 6.12 \times 10^{-5}$ s. The stiffness constants give the natural frequencies of the structural model $f_1 = 100$Hz, $f_2 = 160$Hz, see [13, 14]. The fluid density was $\rho = 1.2$ kg/m$^3$ and the kinematic viscosity $\nu = 1.58 \times 10^{-5}\,\text{m}^2/\text{s}$.

The numerical results are shown in terms of a typical aeroelastic reponse for the aeroelastically unstable system in Fig. 4. The vibration of the vocal fold is shown by the graph of displacements $w_1$ and $w_2$ in time domain. The graph Fig. 4a) corresponds to the phonation onset case, the gap between the vocal folds at the glottis is still wide opened and the modification of the mathematical model to treat the contact phenomena is not needed.

The vocal fold vibrations grows further and the increase of amplitudes finally leads to the almost periodical mutual contact of the vocal folds. The appearance of the impact forces leads to almost a limit cycle of oscillations, see Fig. 4b).

The computations were performed either for the case of porosity coefficient $P$ equal zero (which corresponds to the open space flow) or a prescribed fixed value ($P = 10^6\nu$) of porosity. Figure 6 shows the comparison of these two computations

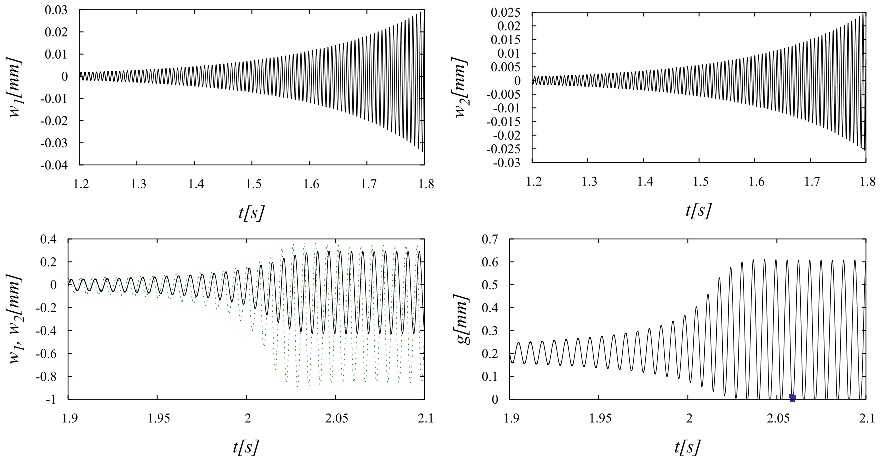


**Fig. 4** The aeroelastic response of the structure for flow velocity $U_\infty = 0.65$ m/s: **a** phonation onset in terms of the displacements $w_1(t)$ and $w_2(t)$ (top), **b** phonation with the glottis closure in terms of the displacements $w_1(t)$ (solid/black line) and $w_2(t)$ (dashed/green line) on the left and the half-gap $g(t)$ on the right

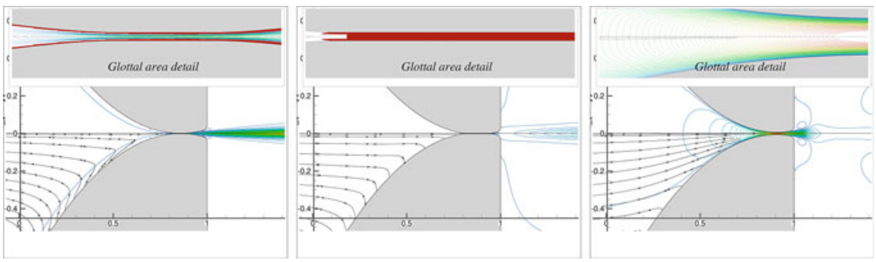


**Fig. 5** The flow patterns in terms of flow velocity magnitude and instantenous streamlines during the closing and the reopening phase. The axis show the non-dimensional coordinates $x/L$, $y/L$ with $L$ being the width of the vocal fold (length in x-direction)

in terms of the inlet quantities. This graph confirms that use of this modified mathematical model also really well addresses the real gap closing similarly as in [7]. The use of the anisotropic porosity has almost no influence on the inlet values of velocity or pressure, see Fig. 6, still the x-component of the gap velocity shown in Fig. 7 becomes zero in the case of the fictitious porosity approach employed. This is also confirmed in Fig. 5, where the flow stops during the closure period (see the middle part of Fig. 5).

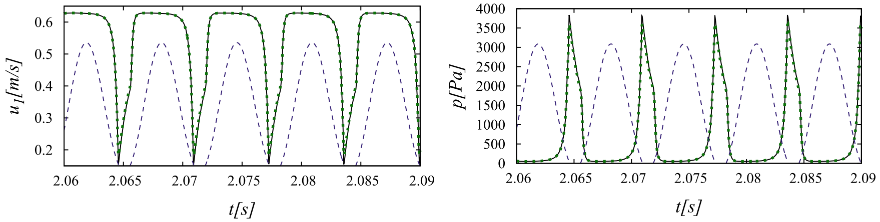


**Fig. 6** Inlet velocity (left) and pressure (right) - comparison of the quantities for zero porosity (dashed/green line) and non-zero porosity (solid/black line). The dotted/blue line shows the (scaled) half-gap in dependence on time

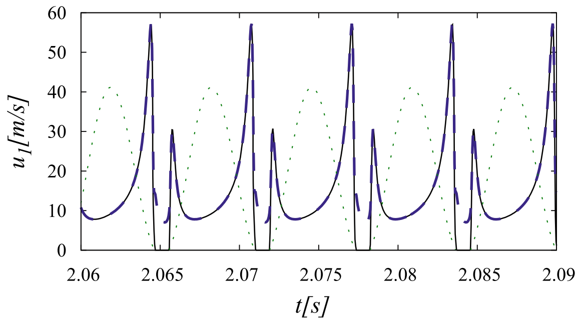


**Fig. 7** The flow velocity x-component in the glottal area - comparison of the results for zero porosity (dashed/blue line) and non-zero porosity (solid/black line). The dotted/green line shows the (scaled) half-gap in dependence on time

# 6 Conclusion

This paper focuse on analysis and an improvement of the mathematical model of human phonation process previously suggested in [7]. The mathematical model is based on the incompressible flow model strongly coupled with a system of ordinary equations describing the motion of the vocal fold model. In order to treat the vocal folds contact the inlet boundary conditions are prescribed by the penalization approach, the geometrical modification of the computational domain is made and in the artificially created part of the computational domain the fictitious anisotropic porous media flow model is used. The analysis of a stationary problem with corresponding boundary conditions is presented. The proposed concept of anisotropic porous media flow is applied , the problem is numerically discretized by an in-house software by the stabilized finite element method. Numerical results are shown proving that the suggested approach is applicable and robust.

## References


1. E.H. Dowell, R.N. Clark, *A modern course in aeroelasticity*. Solid mechanics and its applications (Kluwer Academic Publishers, Dordrecht, Boston, 2004)
2. I.R. Titze, *The Myoelastic Aerodynamic Theory of Phonation* (National Center for Voice and Speech, U.S.A., 2006)
3. J. Horáček, P. Šidlof, J.G. Švec, Journal of Fluids and Structures **20**(6), 853 (2005)
4. J. Valášek, M. Kaltenbacher, P. Sváček, Flow Turbulence Combust **102**, 129–143 (2019)
5. G. Link, M. Kaltenbacher, M. Breuer, M. Döllinger, Computation Methods in Applied Mechanical Engineering **198**, 3321 (2009)
6. K. Ishizaka, J.L. Flanagan, The Bell System Technical Journal **51**, 1233 (1972)
7. P. Sváček, J. Horáček, Journal of Computational and Applied Mathematics **393**, 113529 (2021). https://doi.org/10.1016/j.cam.2021.113529
8. P. Sváček, **61**(SI) (2021)
9. T. Nomura, T.J.R. Hughes, Computer Methods in Applied Mechanics and Engineering **95**, 115 (1992)
10. M. Feistauer, *Mathematical Methods in Fluid Dynamics* (Longman Scientific & Technical, Harlow, 1993)
11. Burman, Erik, Fernández, Miguel A., Frei, Stefan, ESAIM: M2AN **54**(2), 531 (2020). https://doi.org/10.1051/m2an/2019072
12. P. Angot, C.H. Bruneau, P. Fabrie, Numer Math **81** (1999)
13. J. Horáček, J.G. Švec, AMD, American Society of Mechanical Engineers, Applied Mechanics Division **253**(2), 1043 (2002)
14. J. Horáček, J.G. Švec, Journal of Fluids and Structures **16**(7), 931 (2002)
15. P. Sváček, J. Horáček, Communications in Computational Physics **12**(3), 789 (2012)